



An investigation of
OH reactivity with
monaromatics using
GC × GC-TOFMS

R. T. Lidster et al.

This discussion paper is/has been under review for the journal Atmospheric Chemistry and Physics (ACP). Please refer to the corresponding final paper in ACP if available.

The impact of monoaromatic hydrocarbons on OH reactivity in the North Sea boundary layer and free troposphere

R. T. Lidster¹, J. F. Hamilton¹, J. D. Lee^{1,2}, A. C. Lewis^{1,2}, J. R. Hopkins^{1,2}, S. Punjabi¹, A. R. Rickard^{1,2}, and J. C. Young³

¹The Wolfson Atmospheric Chemistry Laboratory, The Chemistry Department, The University of York, Heslington, YO10 5DD, UK

²National Centre for Atmospheric Science, University of York, Heslington, York, UK

³School of Chemistry, University of Leeds, Leeds, LS2 9JT, UK

Received: 31 October 2013 – Accepted: 9 November 2013 – Published: 10 December 2013

Correspondence to: J. F. Hamilton (jacqui.hamilton@york.ac.uk)

Published by Copernicus Publications on behalf of the European Geosciences Union.

Title Page

Abstract

Introduction

Conclusions

References

Tables

Figures



Back

Close

Full Screen / Esc

Printer-friendly Version

Interactive Discussion



Abstract

Reaction with the hydroxyl radical (OH) is the dominant removal mechanism for virtually all volatile organic compounds (VOCs) in the atmosphere, however it can be difficult to reconcile measured OH reactivity with known sinks. Unresolved higher molecular weight VOCs contribute to OH sinks, of which monoaromatics are potentially an important sub-class. A method based on comprehensive two-dimensional gas chromatography coupled to time of flight mass spectrometry (GC × GC-TOFMS) has been developed that extends the degree with which larger VOCs can be individually speciated from whole air samples (WAS). The technique showed excellent sensitivity, resolution and good agreement with an established GC-FID method, for compounds amenable to analysis on both instruments. Measurements have been made of VOCs within the UK east coast marine boundary layer and free troposphere, using samples collected from five aircraft flights in winter 2011. Ten monoaromatic compounds with an array of different alkyl ring substituents have been quantified, in addition to the simple aromatics, benzene, toluene, ethyl benzene and Σm - and p -xylene. These additional compounds were then included into constrained box model simulations of atmospheric chemistry occurring at two UK rural and suburban field sites in order to assess the potential impact of these larger monoaromatics species on OH reactivity; they have been calculated to contribute an additional 2–6% to the overall modelled OH loss rate, providing a maximum additional OH sink of $\sim 0.9 \text{ s}^{-1}$.

1 Introduction

It is well known that the OH radical controls the daylight oxidising capacity of the atmosphere. In the presence of NO_x and VOCs, reactions involving OH can contribute to the formation of a range of important secondary pollutants including tropospheric ozone, NO_2 and secondary organic aerosol (SOA). The [OH] is controlled partly by species emitted from biogenic and anthropogenic sources acting as both precursors and reac-

An investigation of OH reactivity with monaromatics using GC × GC-TOFMS

R. T. Lidster et al.

Title Page

Abstract

Introduction

Conclusions

References

Tables

Figures

⏪

⏩

◀

▶

Back

Close

Full Screen / Esc

Printer-friendly Version

Interactive Discussion

**An investigation of
OH reactivity with
monaromatics using
GC × GC-TOFMS**

R. T. Lidster et al.

Title Page

Abstract

Introduction

Conclusions

References

Tables

Figures

◀

▶

◀

▶

Back

Close

Full Screen / Esc

Printer-friendly Version

Interactive Discussion

tive sinks. Due to the high reactivity of OH ($\tau_{\text{OH}} = 0.01\text{--}1.00\text{ s}$), the effects of air mass transport can be ignored and its concentration is dependant only on the in situ chemical environment and solar irradiance (Logan et al., 1981). In recent years, the in situ measurement of OH reactivity has become a useful tool for assessing our understanding of the reactive sinks for OH in different environments (Kovacs and Brune, 2001; Di Carlo et al., 2004; Sadanaga et al., 2004; Sinha et al., 2008; Nölscher et al., 2012). This is typically performed either by a “pump and probe” (Sadanaga et al., 2004), discharge flow techniques (Kovacs and Brune, 2001; Di Carlo et al., 2004) or by a comparative reactivity method (Sinha et al., 2008; Nölscher et al., 2012). The former uses a laser pulse to generate OH radicals within a reaction cell and, using laser induced fluorescence (LIF), detect the OH concentration decay with time as ambient air is introduced. The discharge flow method differs in the OH generation mechanism, here OH radicals are generated using a mercury UV lamp and injected into a large flow tube with ambient air. The subsequent OH decay is then monitored by LIF. The comparative reactivity method uses a competitive reaction of artificially produced OH radicals with a reagent not typically present in air (e.g pyrrole) (Sinha et al., 2008; Nölscher et al., 2012). The reagent is monitored at three stages (1) before reaction with OH (2) after OH processing and (3) after OH processing in the presence of ambient air. The difference in concentration of the reagent in the presence of, and absence of, ambient air can be attributed to the OH reactivity of that sample.

A total OH reactivity measurement has the advantage of replacing many individual species measurements and includes species which are either not currently measured or are not known. By making comparisons of OH reactivity data with model predictions our current understanding of tropospheric oxidation mechanisms can be tested. Previous reactivity studies have shown that OH loss processes are not fully accounted for, with the in situ measurement of OH reactivity being higher than the sum of all measured individual sinks. Several studies propose that unmeasured species are responsible for the discrepancy. VOCs provide a major loss route for the OH radical in the atmosphere and it has been suggested that unmeasured VOC species may ac-

trace gases including carbon monoxide, ozone, oxides of nitrogen, non-methane hydrocarbons (NMHC), oxygenated volatile organic compounds (OVOC), N₂O₅ and radicals intermediates (NO₃, OH, and HO₂). In addition, aircraft positional data was recorded, along with temperature, pressure, humidity and turbulence.

The FAAM ARA has the facility to accommodate a total of 64 WAS canisters used for collection of air samples during flight. The canisters are 3 L in volume and the interior has been coated with a layer of deactivated silica (silcosteel). The canisters, once fitted into the hold of the aircraft, are filled at various points during flights using an all stainless steel assembly and double headed metal bellows pump. Canisters are typically filled to their maximum fill pressure of 3 atm giving a sample volume of approximately 9 L. The fill pressure is reduced at higher altitudes, but typically always remains above 2 atm. The individual WAS canisters are housed in metal flight cases of between 8 and 15 bottles. Within these cases, bottles are connected together via a common inlet and outlet port. Individual bottles are filled via electronic activation of pneumatic solenoid valves that are controlled by a PC within the aircraft cabin. WAS bottles can be filled at a desired point in the flight or set to automatically fill at regular time intervals using the WAS filling software. All fittings, connectors and gauges used on the WAS case and aircraft assembly are 316 stainless steel to ensure minimal losses and eliminate contamination.

2.2 Gas sampling

A schematic of the instrument setup is shown in Fig. 1. Gas sampling was performed using a Markes Unity 2 with CIA8 (Markes International, Llantrisant, UK) using a general purpose hydrocarbon sorbent trap (Markes International). For WAS samples, the Unity 2 used the following settings. The sorbent trap was cooled to 10 °C and trapping was performed at 100 mL min⁻¹ for 10 min, giving a 1 L sample volume. The trap was then purged for a further 10 min with carrier gas, while maintaining 10 °C, to ensure the majority of trapped water was removed. For injection onto the GC × GC system, the trap was rapidly heated to 250 °C at > 100 °C s⁻¹. The transfer line was heated to

An investigation of OH reactivity with monaromatics using GC × GC-TOFMS

R. T. Lidster et al.

Title Page

Abstract

Introduction

Conclusions

References

Tables

Figures



Back

Close

Full Screen / Esc

Printer-friendly Version

Interactive Discussion



An investigation of OH reactivity with monaromatics using GC × GC-TOFMS

R. T. Lidster et al.

Title Page

Abstract

Introduction

Conclusions

References

Tables

Figures

⏪

⏩

◀

▶

Back

Close

Full Screen / Esc

Printer-friendly Version

Interactive Discussion



After sampling and desorption, the flow is split 50 : 50 and passes down a aluminium oxide (Al_2O_3) Porous Layer Open Tubular (PLOT) column (50 m, 0.53 mm id) for analysis of NMHCs and two LOWOX columns (10 m, 0.53 mm id) in series for analysis of OVOCs. The instrument setup and operation is described in detail in Hopkins et al. (2006, 2011). Calibrations were performed using a 30 component ppbv level ozone precursor standard, NPL30 (National Physics Laboratory).

3 Results and discussion

The GC × GC-TOFMS system was calibrated using a series of gas standards and an example chromatogram is shown in Fig. 2, where the retention times in columns 1 and 2 are shown on the x- and y-axes respectively and the peak intensity shown as a coloured contour. The instrument shows excellent separation of the hydrocarbons with $>\text{C}_5$, with the exception of *m/p*-xylene as seen in most GC separations using siloxane columns. No signals were seen for hydrocarbons with less than 5 carbons as they were too volatile to be retained on the liquid nitrogen modulator. An advantage of GC × GC is that compounds elute in characteristic patterns depending on their functionality. This pattern can be observed in Fig. 2 with the aromatic species well separated from the aliphatics in the second dimension. Precision, limits of detection (LOD) and linearity of calibration for the species calibrated using gas standards are shown in Table 1. The relative standard deviation was calculated for 5 replicate injections of a 1 L sample of the AR74 hydrocarbon standard at ~ 100 pptv and the R^2 value given is for a 6 point calibration ranging from approximately 10 pptv to 250 pptv (depending on the standard mixing ratio of each compound). The limit of detection was calculated at $S/N = 3$. The retention time and quantification ion used for the calibration are also shown.

The GC × GC-TOFMS was able to consistently resolve the majority of species in the gas standard with relative standard deviation (%RSD) values less than 5 %, with the exception of 1-pentene, cis-2-pentene and 2-methyl-2-butene that gave a higher %RSD. These compounds co-elute with each other on the column set used and have similar

Fig. 5. This can be rationalised due to their similar emission sources (i.e. petrol vapours and evaporation). The alkyl benzenes generally have the same emission sources and so the gradient of the regression line is a result of both emission ratios and reactivity with atmospheric oxidants encountered by the air mass from emission to sampling, assuming the same dilution rate. The higher MW aromatic species may be atmospherically relevant (Hamilton and Lewis, 2003) as many of them exhibit an enhanced reaction rate over toluene with OH and NO₃ radicals (Atkinson and Arey, 2003) and thus they could impact tropospheric ozone formation rates.

The strong linear relationships observed by the GC × GC-TOFMS presents an opportunity to predict the heavier mono-aromatic VOC loading by measurement of a toluene mixing ratio alone. This would potentially allow techniques that cannot analyse these species (GC-FID, PTR-MS etc) to make a prediction of the additional aromatic content. For the correlation plots presented in Fig. 5, the intercept in each was set to zero. In order to make a meaningful prediction of the additional aromatic content, a conversion that reflects each aromatic species' concentration and rate of reaction with an atmospheric oxidant is required. This was performed by converting the mixing ratio of each aromatic species into a Toluene Equivalent mixing ratio, [J_{Tol}]. This technique has been used previously in the literature (as a propylene equivalent) to allow atmospheric modellers to simplify VOC data and express it as one variable (Chameides et al., 1992). The conversion of a mixing ratio into a [J_{Tol}] value is performed by multiplying the mixing ratio of the aromatic [x], by the ratio of its rate constant, $k_{\text{OH}}(x)$, to that of toluene, $k_{\text{OH}}(\text{Toluene})$ as shown in Eq. (1).

$$[J_{\text{Tol}}] = [x] \frac{k_{\text{OH}}(x)}{k_{\text{OH}}(\text{Toluene})} \quad (1)$$

After conversion of the additional aromatic species into a [J_{Tol}], the relationship between the toluene mixing ratio and the additional aromatic loading as a [J_{Tol}] value was investigated. For all samples analysed using the GC × GC-TOFMS, the mixing ratios of the ten additional aromatic species (Table 2 shown in bold) were converted to a [J_{Tol}]

An investigation of OH reactivity with monaromatics using GC × GC-TOFMS

R. T. Lidster et al.

Title Page

Abstract

Introduction

Conclusions

References

Tables

Figures

⏪

⏩

◀

▶

Back

Close

Full Screen / Esc

Printer-friendly Version

Interactive Discussion



value with respect to both reaction with OH, ($[J_{\text{Tot}}]_{\text{OH}}$) and NO_3 ($[J_{\text{Tot}}]_{\text{NO}_3}$) since many of the samples were taken at night and aromatic reactivity with O_3 is negligible.

As no rate data is currently available in the literature, rate constants for the reactions of 1,3-diethyl benzene and 1,4-diethyl benzene have been calculated using available Structure Activity Relationships (SARs). The SAR approach of Kwok and Atkinson (1995) has been used to estimate total k_{OH} for each diethyl benzene isomer from calculations of partial OH rate constants for hydrogen abstraction from the ethyl groups and OH addition to the aromatic ring. Rate coefficients for OH-addition to the ring are estimated from a correlation of the sum of electrophilic substituent constants (Brown and Okamoto, 1958) with measured OH addition rate constants (Calvert et al., 2002). Rate constants for reaction with NO_3 (k_{NO_3}) have been inferred from measured rate data for *m*- and *p*-xylenes (Calvert et al., 2002) using the method applied by Jenkin et al. (2003). As with all estimation methods, there is a reasonable error of uncertainty and as such an error of a factor of 2 should be applied (Kwok and Atkinson, 1995).

The $[J_{\text{Tot}}]$ values of the 10 individual compounds were then summed for each sample to give a $\Sigma[J_{\text{Tot}}]$, that represents the additional aromatics measured at each sampling point. The $\Sigma[J_{\text{Tot}}]$ values were plotted against their respective toluene mixing ratio and are shown in Fig. 6. A reasonable linear relationship is seen with an R^2 of 0.93 and a gradient of 2.03 and 7.30 for OH and NO_3 respectively.

The ten additional monocyclic aromatics may have a considerable effect on reactivity and also potentially ozone formation with a $[J_{\text{Tot}}]_{\text{OH}}$ that is on average twice that of the toluene mixing ratio.

The average contribution of each aromatic species to the $\Sigma[J_{\text{Tot}}]$ value can be observed Fig. 7. The tri-substituted benzenes, although at a significantly lower mixing ratio than toluene (average mixing ratio for 1,3,5 trimethylbenzene is 4.7 pptv c.f. toluene which is 136.7 pptv), exhibit a significant rate enhancement for reaction with OH (Fig. 7a) and so give rise to large $[J_{\text{Tot}}]$ values. In contrast to OH, the NO_3 radical exhibits a slower rate of reaction with toluene and other aromatic species. However the

An investigation of OH reactivity with monaromatics using GC × GC-TOFMS

R. T. Lidster et al.

Title Page

Abstract

Introduction

Conclusions

References

Tables

Figures

⏪

⏩

◀

▶

Back

Close

Full Screen / Esc

Printer-friendly Version

Interactive Discussion

additional aromatic content still adds a large portion of $\Sigma[J_{\text{Tot}}]_{\text{NO}_3}$ when compared to the toluene mixing ratio alone, as shown in Fig. 7b.

A range of different locations off the East and South coast of the UK were sampled during the 5 RONOCO flights. A summary of the flight tracks and vertical distribution of total $[J_{\text{Tot}}]_{\text{OH}}$ from the aircraft WAS bottles can be observed in Fig. 8. This shows an expected reduction in reactive toluene equivalent with altitude. Variation at lower altitudes is the result of differential plume sampling.

The FGAM-DC-GC-FID used in this study exhibits reduced performance when analysing these aromatic species due to poor peak shape and increased co-elution, which contribute to a higher limit of detection. Using the gradients of linear regressions from the measured GC \times GC-TOFMS data and the toluene mixing ratio from the FGAM GC-FID, a prediction of the $\Sigma[J_{\text{Tot}}]$ value was carried out. The predicted additional aromatic $\Sigma[J_{\text{Tot}}]$ calculated using the FGAM-GC-FID toluene mixing ratio is shown by the blue line in Fig. 6. The additional aromatic content calculated using the proportionality factors shows a good level of agreement with the measured values, with a discrepancy between the two trend lines of approximately $< 0.4\%$ for both radical oxidants. The correlation data for each additional aromatic species can be found in Table 3 along with its corresponding R^2 value for the linear regression. The 2002 UK National Emission Inventory (NEI) ratios to toluene are also presented for comparison.

The short daytime lifetimes of these larger molecular weight monoaromatics means the observed daytime ratio to toluene is likely to change depending on the sample's distance from source. The RONOCO flights address this issue as they took place at night (or dawn) resulting in the air mass sampled containing well mixed source material with minimal OH losses. Many of the samples collected in this study were taken off the coast of the UK, (North Sea and the English Channel) providing a well mixed, integrated assessment of the reactive higher VOC to toluene ratio. This is in contrast to surface measurements that can sometimes be affected by localised sources.

An investigation of OH reactivity with monaromatics using GC \times GC-TOFMS

R. T. Lidster et al.

Title Page

Abstract

Introduction

Conclusions

References

Tables

Figures

⏪

⏩

◀

▶

Back

Close

Full Screen / Esc

Printer-friendly Version

Interactive Discussion



An investigation of OH reactivity with monaromatics using GC × GC-TOFMS

R. T. Lidster et al.

Title Page

Abstract

Introduction

Conclusions

References

Tables

Figures

◀

▶

◀

▶

Back

Close

Full Screen / Esc

Printer-friendly Version

Interactive Discussion



that many of the higher molecular weight aromatics exhibited a strong correlation with toluene, indicating similar anthropogenic sources. Assuming this relationship is consistent, the use of the proportionality factors ($[J_{\text{Tot}}]$) obtained here can be used to predict the mixing ratios of these additional aromatic species without needing to measure them directly. Adding ten previously unaccounted for monoaromatic compounds to model simulations of both polluted and rural chemistry increased the total simulated OH reactivity by up to 6 %, bring the modelled OH reactivity more into line with the measurements. The proportionality factors were determined using VOC measurements taken under a range of different air masses, from localised pollution to aged regional background and so should be typical for the UK. However more work is needed to study whether these scaling factors are consistent at other locations.

Quantification of many of the species detected within this study was not possible owing to a lack of appropriate standards and unknown stability within the WAS canisters. Their impact is also uncertain since in many cases kinetic data is not available. GC × GC-TOFMS has the ability to detect and resolve many other functionalities of atmospherically relevant species such as higher MW multifunctional volatile oxygenates, halocarbons and alkyl nitrates shown in Fig. 10. In the future it would be possible to develop an atmospheric sampling method that has the potential to target all these species, within a single analysis, if standards for these species were available.

References

- Atkinson, R. and Arey, J.: Gas-phase tropospheric chemistry of biogenic volatile organic compounds: a review, *Atmos. Environ.*, 37, 197–219, 2003. 32434
- Bartenbach, S., Williams, J., Plass-Dülmer, C., Berresheim, H., and Lelieveld, J.: In-situ measurement of reactive hydrocarbons at Hohenpeissenberg with comprehensive two-dimensional gas chromatography (GC × GC-FID): use in estimating HO and NO₃, *Atmos. Chem. Phys.*, 7, 1–14, doi:10.5194/acp-7-1-2007, 2007. 32426
- Brown, H. C. and Okamoto, Y.: Electrophilic substituent constants, *J. Am. Chem. Soc.*, 80, 4979–4987, doi:10.1021/ja01551a055, 1958. 32435

**An investigation of
OH reactivity with
monaromatics using
GC × GC-TOFMS**

R. T. Lidster et al.

Title Page

Abstract

Introduction

Conclusions

References

Tables

Figures

◀

▶

◀

▶

Back

Close

Full Screen / Esc

Printer-friendly Version

Interactive Discussion

Calvert, J. G., Atkinson, R., Becker, K. H., Kamens, R. M., Seinfeld, J. H., Wallington, T. J., and Yarwood, G.: The Mechanisms of Atmospheric Oxidation of Aromatic Hydrocarbons, Oxford University Press, 2002. 32435

Chameides, W. L., Fehsenfeld, F., Rodgers, M. O., Cardelino, C., Martinez, J., Parrish, D., Lonnenman, W., Lawson, D. R., Rasmussen, R. A., Zimmerman, P., Greenberg, J., Middleton, P., and Wang, T.: Ozone precursor relationships in the ambient atmosphere, *J. Geophys. Res.*, 97, 6037–6055, 1992. 32434

Di Carlo, P., Brune, W. H., Martinez, M., Harder, H., Leshner, R., Ren, X., Thornberry, T., Carroll, M. A., Young, V., Shepson, P. B., Riemer, D., Apel, E., and Campbell, C.: Missing OH Reactivity in a Forest: Evidence for unknown reactive biogenic VOCs, *Science*, 304, 722–725, doi:10.1126/science.1094392, 2004. 32425, 32426, 32437

Emmerson, K. M., Carslaw, N., Carslaw, D. C., Lee, J. D., McFiggans, G., Bloss, W. J., Gravestock, T., Heard, D. E., Hopkins, J., Ingham, T., Pilling, M. J., Smith, S. C., Jacob, M., and Monks, P. S.: Free radical modelling studies during the UK TORCH Campaign in Summer 2003, *Atmos. Chem. Phys.*, 7, 167–181, doi:10.5194/acp-7-167-2007, 2007. 32437, 32438

Goldstein, A. H. and Galbally, I. E.: Known and unexplored organic constituents in the earth's atmosphere, *Environ. Sci. Technol.*, 41, 1514–1521, 2007. 32426, 32432

Hamilton, J. F. and Lewis, A. C.: Monoaromatic complexity in urban air and gasoline assessed using comprehensive GC and fast GC-TOF/MS, *Atmos. Environ.*, 37, 589–602, 2003. 32434

Hopkins, J. R., Boddy, R. K., Hamilton, J. F., Lee, J. D., Lewis, A. C., Purvis, R. M., and Watson, N. J.: An observational case study of ozone and precursors inflow to South East England during an anticyclone, *J. Environ. Monit.*, 8, 1195–1202, 2006. 32431

Hopkins, J. R., Jones, C. E., and Lewis, A. C.: A dual channel gas chromatograph for atmospheric analysis of volatile organic compounds including oxygenated and monoterpene compounds, *J. Environ. Monit.*, 13, 2268–2276, 2011. 32431

Ingham, T., Goddard, A., Whalley, L. K., Furneaux, K. L., Edwards, P. M., Seal, C. P., Self, D. E., Johnson, G. P., Read, K. A., Lee, J. D., and Heard, D. E.: A flow-tube based laser-induced fluorescence instrument to measure OH reactivity in the troposphere, *Atmos. Meas. Tech.*, 2, 465–477, doi:10.5194/amt-2-465-2009, 2009. 32438

Jenkin, M. E., Saunders, S. M., Wagner, V., and Pilling, M. J.: Protocol for the development of the Master Chemical Mechanism, MCM v3 (Part B): tropospheric degradation of aromatic volatile organic compounds, *Atmos. Chem. Phys.*, 3, 181–193, doi:10.5194/acp-3-181-2003, 2003. 32435

**An investigation of
OH reactivity with
monaromatics using
GC × GC-TOFMS**

R. T. Lidster et al.

Title Page

Abstract

Introduction

Conclusions

References

Tables

Figures

⏪

⏩

◀

▶

Back

Close

Full Screen / Esc

Printer-friendly Version

Interactive Discussion



- Kovacs, T. and Brune, W.: Total OH loss rate measurement, *J. Atmos. Chem.*, 39, 105–122, doi:10.1023/A:1010614113786, 2001. 32425
- Kwok, E. S. C. and Atkinson, R.: Estimation of hydroxyl radical reaction-rate constants for gas-phase organic-compounds using a structure-reactivity relationship – an update, *Atmos. Environ.*, 29, 1685–1695, 1995. 32435
- 5 Lee, J., Young, J., Read, K., Hamilton, J., Hopkins, J., Lewis, A., Bandy, B., Davey, J., Edwards, P., Ingham, T., Self, D., Smith, S., Pilling, M., and Heard, D.: Measurement and calculation of OH reactivity at a United Kingdom coastal site, *J. Atmos. Chem.*, 64, 53–76, 2009. 32426, 32437, 32438
- 10 Lee, J. D., Lewis, A. C., Monks, P. S., Jacob, M., Hamilton, J. F., Hopkins, J. R., Watson, N. M., Saxton, J. E., Ennis, C., Carpenter, L. J., Carslaw, N., Fleming, Z., Bandy, B. J., Oram, D. E., Penkett, S. A., Slemr, J., Norton, E., Rickard, A. R., Whalley, L., Heard, D. E., Bloss, W. J., Gravestock, T., Smith, S. C., Stanton, J., Pilling, M. J., and Jenkin, M. E.: Ozone photochemistry and elevated isoprene during the UK heatwave of august 2003, *Atmos. Environ.*, 40, 7598–7613, 2006. 32426, 32437
- 15 Lewis, A. C., Carslaw, N., Marriott, P. J., Kinghorn, R. M., Morrison, P., Lee, A. L., Bartle, K. D., and Pilling, M. J.: A larger pool of ozone-forming carbon compounds in urban atmospheres, *Nature*, 405, 778–781, 2000. 32426
- Logan, J. A., Prather, M. J., Wofsy, S. C., and McElroy, M. B.: Tropospheric chemistry: a global perspective, *J. Geophys. Res.*, 86, 7210–7254, 1981. 32425
- 20 Mao, J., Ren, X., Brune, W. H., Olson, J. R., Crawford, J. H., Fried, A., Huey, L. G., Cohen, R. C., Heikes, B., Singh, H. B., Blake, D. R., Sachse, G. W., Diskin, G. S., Hall, S. R., and Shetter, R. E.: Airborne measurement of OH reactivity during INTEX-B, *Atmos. Chem. Phys.*, 9, 163–173, doi:10.5194/acp-9-163-2009, 2009. 32426, 32437
- 25 Nölscher, A. C., Sinha, V., Bockisch, S., Klüpfel, T., and Williams, J.: Total OH reactivity measurements using a new fast Gas Chromatographic Photo-Ionization Detector (GC-PID), *Atmos. Meas. Tech.*, 5, 2981–2992, doi:10.5194/amt-5-2981-2012, 2012. 32425
- Phillips, J. and Liu, Z.: Comprehensive two-dimensional gas chromatography using an on-column thermal modulator interface, *J. Chromatogr. Sci.*, 28, 227–231, 1991. 32426
- 30 Sadanaga, Y., Yoshino, A., Watanabe, K., Yoshioka, A., Wakazono, Y., Kanaya, Y., and Kajii, Y.: Development of a measurement system of OH reactivity in the atmosphere by using a laser-induced pump and probe technique, *Rev. Sci. Instrum.*, 75, 2648–2655, doi:10.1063/1.1775311, 2004. 32425, 32437

**An investigation of
OH reactivity with
monaromatics using
GC × GC-TOFMS**

R. T. Lidster et al.

Title Page

Abstract

Introduction

Conclusions

References

Tables

Figures

◀

▶

◀

▶

Back

Close

Full Screen / Esc

Printer-friendly Version

Interactive Discussion

- Saxton, J. E., Lewis, A. C., Kettlewell, J. H., Ozel, M. Z., Gogus, F., Boni, Y., Korogone, S. O. U., and Serça, D.: Isoprene and monoterpene measurements in a secondary forest in northern Benin, *Atmos. Chem. Phys.*, 7, 4095–4106, doi:10.5194/acp-7-4095-2007, 2007. 32426
- Sinha, V., Williams, J., Crowley, J. N., and Lelieveld, J.: The Comparative Reactivity Method – a new tool to measure total OH Reactivity in ambient air, *Atmos. Chem. Phys.*, 8, 2213–2227, doi:10.5194/acp-8-2213-2008, 2008. 32425
- Sinha, V., Williams, J., Lelieveld, J., Ruuskanen, T., Kajos, M., Patokoski, J., Hellen, H., Hakola, H., Mogensen, D., Boy, M., Rinne, J., and Kulmala, M.: OH reactivity measurements within a boreal forest: evidence for unknown reactive emissions, *Environ. Sci. Technol.*, 44, 6614–6620, doi:10.1021/es101780b, 2010. 32437
- Stone, D., Whalley, L. K., and Heard, D. E.: Tropospheric OH and HO₂ radicals: field measurements and model comparisons, *Chem. Soc. Rev.*, 41, 6348–6404, doi:10.1039/C2CS35140D, 2012. 32437
- Xu, X., Stee, L. L. P., Williams, J., Beens, J., Adahchour, M., Vreuls, R. J. J., Brinkman, U. A., and Lelieveld, J.: Comprehensive two-dimensional gas chromatography (GC × GC) measurements of volatile organic compounds in the atmosphere, *Atmos. Chem. Phys.*, 3, 665–682, doi:10.5194/acp-3-665-2003, 2003a. 32426
- Xu, X., Williams, C., Plass-Dülmer, H., Berresheim, H., Salisbury, G., Lange, L., and Lelieveld, J.: GC × GC measurements of C₇-C₁₁ aromatic and n-alkane hydrocarbons on Crete, in air from Eastern Europe during the MINOS campaign, *Atmos. Chem. Phys.*, 3, 1461–1475, doi:10.5194/acp-3-1461-2003, 2003b. 32426

An investigation of OH reactivity with monaromatics using GC × GC-TOFMS

R. T. Lidster et al.

Title Page

Abstract

Introduction

Conclusions

References

Tables

Figures

⏪

⏩

◀

▶

Back

Close

Full Screen / Esc

Printer-friendly Version

Interactive Discussion



Table 1. Continued.

Compound	RT (1D/s, 2D/s)	Quant Mass	%RSD ^a	LOD/pptv ^b	R^{2c}	Figure ref
Aromatics						
Benzene	548, 0.700	78.00	3.58	0.01	0.9994	2 – 22
Toluene	900, 0.960	91.00	5.53	0.03	0.9997	2 – 37
Ethyl benzene	1260, 1.130	91.00	3.57	0.03	0.9997	2 – 38
m/p-xylene	1294, 1.130	91.00	3.36	0.05	0.9993	2 – 39
o-xylene	1388, 1.230	91.00	4.05	0.03	0.9982	2 – 40
Styrene	1390, 1.320	104.00	1.16	0.04	0.9965	2 – 41
Benzene, isopropyl-	1500, 1.170	105.00	2.99	0.02	0.9996	2 – 42
Benzene, propyl-	1616, 1.210	91.00	3.22	0.02	0.9999	2 – 43
Toluene, 3-ethyl-	1642, 1.230	105.00	2.76	0.02	0.9995	2 – 44
Toluene, 4-ethyl-	1658, 1.210	105.00	4.76	0.02	0.9994	2 – 45
Benzene, 1,3,5 trimethyl-	1674, 1.220	105.00	3.78	0.02	0.9991	2 – 46
Toluene, 2-ethyl-	1714, 1.320	105.00	5.01	0.02	0.9997	2 – 47
Benzene, t-butyl-	1758, 1.230	91.00	3.75	0.03	0.9986	2 – 48
Benzene, 1,2,4 trimethyl-	1774, 1.300	105.00	4.88	0.02	0.9992	2 – 49
Benzene, 1,2,3 trimethyl-	1882, 1.440	105.00	3.07	0.03	0.9958	2 – 50
Benzene, 1,3-diethyl-	1958, 1.310	105.00	5.18	0.05	0.9993	2 – 51
Benzene, 1,4-diethyl-	1996, 1.290	105.00	3.47	0.06	0.9995	2 – 52
Indane	1948, 1.600	117.00	2.59	0.02	0.9971	2 – 53
Terpenes						
Isoprene	254, 0.120	67.00	1.24	0.07	0.9986	2 – 5
α -Pinene	1528, 0.920	93.00	0.87	0.08	0.9975	–
β -Pinene	1712, 1.090	93.00	3.96	0.11	0.9956	–
3-Carene	1814, 1.110	93.00	3.44	0.11	0.9960	–
Limonene	1892, 1.140	67.00	2.68	0.11	0.9980	–
Eucalyptol	1916, 1.240	81.00	1.88	0.10	0.9939	–

^a % RSD is taken from 5 replicates

^b The Limit of Detection (LOD) is taken at $S/N = 3$

^c R^2 value from a 6 point calibration with mixing ratios ranging from ~ 10 pptv to 250 pptv for a 1 L sample

Table 2. VOC Mixing ratios measured by GC × GC-TOFMS during the Winter RONOCO campaign for all samples taken.

Compound	RT (1D/s, 2D/s)	LOD/ pptv	Mean/ pptv	Median/ pptv	MAD ^a / pptv	Min ^b / pptv	Max ^c / pptv
Alkanes							
Pentane	242, 0.060	0.13	133.1	86.4	27.4	10.2	3213.9
Butane, 2,2-dimethyl-	278, 0.070	0.04	8.8	7.5	3.4	0.36	55.2
Pentane, 2-methyl-	320, 0.130	0.03	27.3	19.6	8.3	1.3	505.0
Pentane, 3-methyl-	346, 0.160	0.04	32.2	25.3	10.5	1.8	421.9
Hexane	374, 0.180	0.05	50.4	36.8	12.6	4.9	838.1
Pentane, 2,4-dimethyl-	432, 0.210	0.04	4.5	3.7	1.6	0.09	41.7
Cyclopentane, methyl-	450, 0.310	0.04	29.5	21.2	8.9	1.1	515.4
Hexane, 2-methyl-	528, 0.280	0.06	13.9	11.2	4.1	0.95	142.2
Pentane, 2,3-dimethyl-	542, 0.300	0.08	7.5	5.9	2.5	0.41	78.1
Cyclohexane	544, 0.430	0.28	18.8	14.2	5.2	0.95	286.1
Hexane, 3-methyl-	556, 0.310	0.06	17.8	14.0	5.6	1.2	186.0
Heptane	628, 0.350	0.08	29.0	21.7	8.5	2.4	358.5
Cyclohexane, methyl-	736, 0.520	0.03	18.4	12.0	5.2	0.22	320.7
Pentane, 2,3,4-trimethyl-	804, 0.450	0.04	4.0	3.7	1.8	0.15	12.1
Heptane, 2/4-methyl-	850, 0.430	0.07	11.4	8.9	4.0	0.48	109.8
Heptane, 3-methyl-	880, 0.460	0.05	4.3	3.6	1.7	0.24	30.0
Octane	980, 0.490	0.09	9.8	7.6	3.1	1.0	78.4
Nonane	1362, 0.610	0.05	10.2	7.8	3.7	0.33	48.8
Decane	1738, 0.700	0.05	15.9	12.3	4.9	0.62	59.7
Undecane	2094, 0.780	0.08	17.4	14.1	4.9	0.12	52.8
Alkenes							
1-Pentene, 2-methyl-	358, 0.200	0.05	5.6	3.4	1.7	0.40	126.9
Cyclohexene	596, 0.560	0.04	0.7	0.6	0.29	0.13	3.5
1-Heptene	606, 0.390	0.09	12.6	8.6	3.4	0.40	261.2
Styrene	1390, 1.320	0.04	11.2	14.9	4.0	0.65	65.19
Aromatics							
Benzene	548, 0.700	0.01	151.5	144.3	27.8	66.5	435.3
Toluene	900, 0.960	0.03	136.7	107.9	47.6	7.8	808.7
Ethyl benzene	1260, 1.130	0.03	25.9	21.3	10.1	1.2	157.0
m/p-Xylene	1294, 1.130	0.05	70.6	58.8	31.2	3.6	264.0
o-Xylene	1388, 1.230	0.03	23.3	19.1	9.9	0.91	90.2
Benzene, isopropyl-	1500, 1.170	0.02	1.5	1.3	0.54	0.08	5.4
Benzene, propyl-	1616, 1.210	0.02	4.7	3.1	1.4	0.09	25.7
Toluene, 3-ethyl-	1642, 1.230	0.02	11.4	8.2	4.0	0.31	53.5
Toluene, 4-ethyl-	1658, 1.210	0.02	5.7	4.2	2.0	0.11	26.4
Benzene, 1,3,5 trimethyl-	1674, 1.220	0.02	4.7	3.4	1.7	0.11	20.2
Toluene, 2-ethyl-	1714, 1.320	0.02	5.3	3.9	1.8	0.10	23.9
Benzene, 1,2,4 trimethyl-	1774, 1.300	0.02	15.8	11.5	6.0	1.0	71.5
Benzene, 1,2,3 trimethyl-	1882, 1.440	0.03	4.2	3.1	1.4	0.38	17.2
Benzene, 1,3-diethyl-	1958, 1.310	0.05	1.0	0.80	0.50	0.16	3.9
Benzene, 1,4-diethyl-	1996, 1.290	0.06	2.6	2.0	1.0	0.19	9.5

^a The median absolute deviation

^b Minimum mixing ratio measured

^c Maximum mixing ratio measured

Bold = Additional aromatic species featured in this additional reactivity study

An investigation of
OH reactivity with
monaromatics using
GC × GC-TOFMS

R. T. Lidster et al.

Title Page

Abstract

Introduction

Conclusions

References

Tables

Figures



Back

Close

Full Screen / Esc

Printer-friendly Version

Interactive Discussion



An investigation of OH reactivity with monaromatics using GC × GC-TOFMS

R. T. Lidster et al.

Title Page

Abstract

Introduction

Conclusions

References

Tables

Figures

⏪

⏩

◀

▶

Back

Close

Full Screen / Esc

Printer-friendly Version

Interactive Discussion

Table 3. The scaling factors for the 10 additional aromatic species against toluene along with there corresponding R^2 values from the linear regressions in Fig. 5. The 2002 NEI ratio to toluene for comparison.

Species	Slope of Regression	R^2	NEI 2002 ratio to toluene
Benzene, isopropyl	0.0121x	0.9220	0.0083
Benzene, propyl-	0.0374x	0.8457	0.0279
Toluene, 3-ethyl-	0.0996x	0.8497	0.0250
Toluene, 4-ethyl-	0.0501x	0.8446	0.0102
Benzene, 1,3,5-trimethyl-	0.0397x	0.8471	0.1025
Toluene, 2-ethyl-	0.0462x	0.8473	0.0002
Benzene, 1,2,4-trimethyl-	0.1357x	0.8269	0.2749
Benzene, 1,2,3-trimethyl-	0.0349x	0.8410	0.0776
Benzene, 1,3-diethyl-	0.0076x	0.6572	0.0067
Benzene, 1,4-diethyl-	0.0203x	0.7314	0.0068

An investigation of OH reactivity with monaromatics using GC × GC-TOFMS

R. T. Lidster et al.

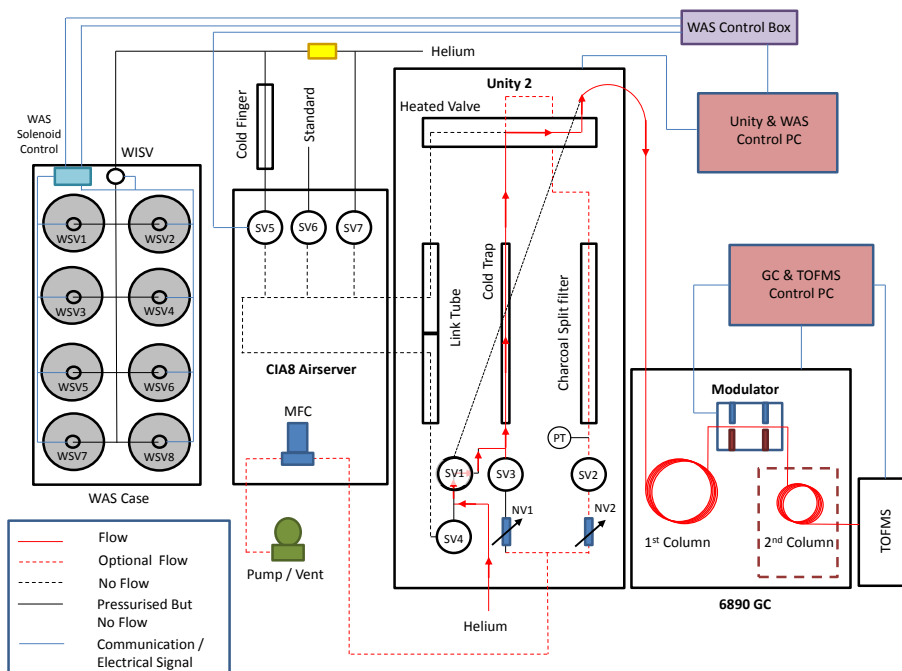


Fig. 1. Schematic of the finalised TD-GC × GC-TOFMS sampling set-up. SV = solenoid valve. NV = Needle valve. MFC = Mass flow controller. WISV = WAS inlet solenoid valve. WSV = WAS solenoid valve. PT = Pressure transducer.

Title Page	
Abstract	Introduction
Conclusions	References
Tables	Figures
◀	▶
◀	▶
Back	Close
Full Screen / Esc	
Printer-friendly Version	
Interactive Discussion	

An investigation of OH reactivity with monaromatics using GC × GC-TOFMS

R. T. Lidster et al.

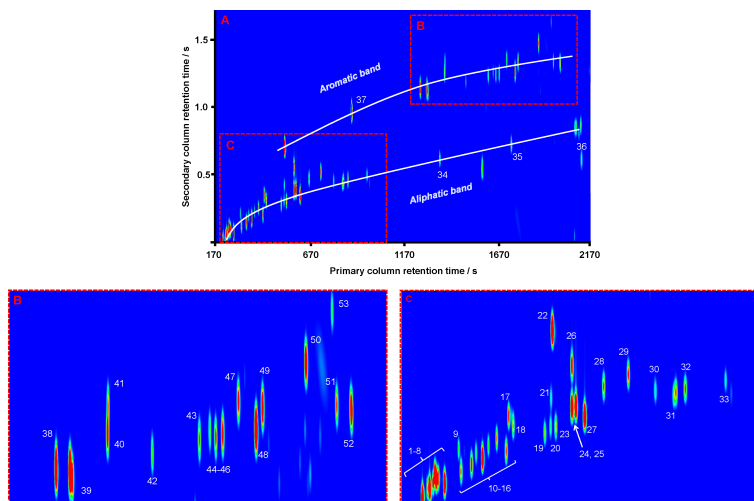


Fig. 2. (A) TD-GC × GC-TOFMS chromatogram of the AR74 HC standard. Labeled peaks are identified as follows: (34) nonane; (35) decane; (36) undecane and (37) toluene. Box (B) shows the aromatic region of the chromatogram. Labeled peaks are identified as follows: (38) ethyl benzene; (39) m/p-xylene; (40) o-xylene; (41) styrene; (42) isopropyl benzene; (43) propyl benzene; (44) 3-ethyltoluene; (45) 4-ethyltoluene; (46) 1,3,5-trimethylbenzene; (47) 2-ethyl toluene; (48) t-butylbenzene; (49) 1,2,4-trimethylbenzene; (50) 1,2,3-trimethylbenzene; (51) 1,3-diethylbenzene; (52) 1,4-diethylbenzene and (53) indane. Box (C) shows the aliphatic region. Labeled peaks are identified as follows: (1) 2-methylbutane; (2) pentane; (3) 1-pentene; (4) E-2-pentene; (5) isoprene; (6) Z-2-pentene; (7) 2-methyl-2-butene; (8) 2,2-dimethylbutane; (9) cyclopentene; (10) 2-methylpentane; (11) 3-methylpentane; (12) 2-methyl-1-pentene; (13) hexane; (14) E-2-hexene; (15) Z-2-hexene; (16) 2,4-dimethylpentane; (17) 1,3-hexadiene; (18) methylcyclopentane; (19) 2-methylhexane; (20) 2,3-dimethylpentane (21) cyclohexane; (22) benzene; (23) 3-methylhexane; (24) 1,3-dimethylcyclopentane (25) 1-heptene; (26) cyclohexene; (27) heptane; (28) 2,3-dimethyl-2-pentene; (29) methylcyclohexane; (30) 2,3,4-trimethylpentane; (31) 2/4-methylheptane; (32) 3-methylheptane and (33) octane.

Title Page

Abstract Introduction

Conclusions References

Tables Figures

◀ ▶

◀ ▶

Back Close

Full Screen / Esc

Printer-friendly Version

Interactive Discussion

An investigation of OH reactivity with monaromatics using GC × GC-TOFMS

R. T. Lidster et al.

Title Page

Abstract

Introduction

Conclusions

References

Tables

Figures



Back

Close

Full Screen / Esc

Printer-friendly Version

Interactive Discussion

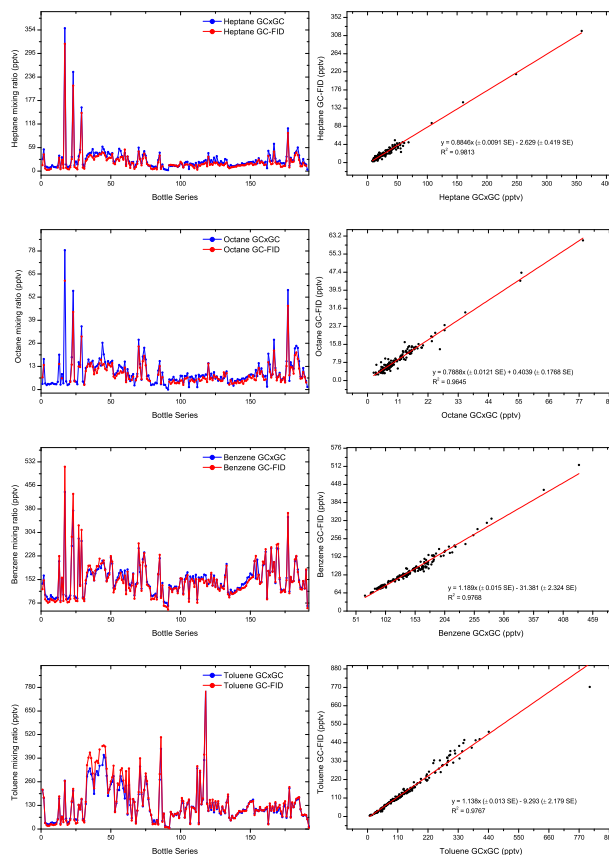


Fig. 3. Inter-comparison data for selected compounds measured by both GC × GC-TOFMS and GC-FID.

An investigation of OH reactivity with monaromatics using GC × GC-TOFMS

R. T. Lidster et al.

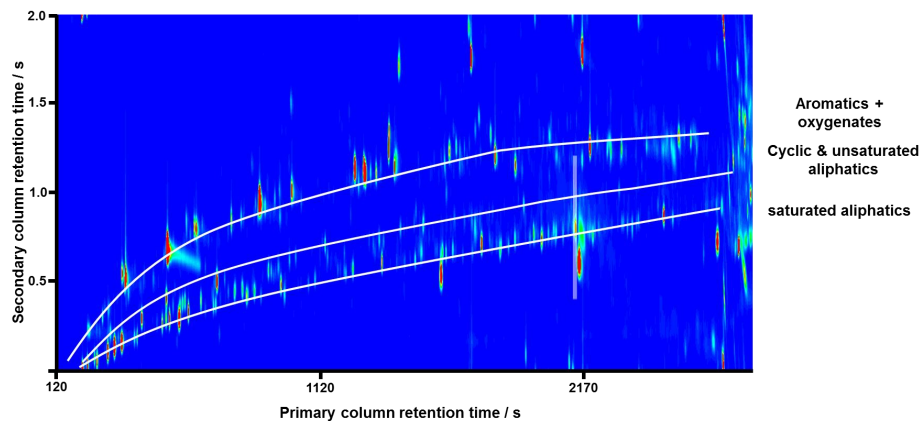


Fig. 4. Typical GC × GC-TOFMS chromatogram from RONOCO highlighting the functional group pattern formation.

[Title Page](#)[Abstract](#)[Introduction](#)[Conclusions](#)[References](#)[Tables](#)[Figures](#)[⏪](#)[⏩](#)[◀](#)[▶](#)[Back](#)[Close](#)[Full Screen / Esc](#)[Printer-friendly Version](#)[Interactive Discussion](#)

An investigation of OH reactivity with monaromatics using GC × GC-TOFMS

R. T. Lidster et al.

Title Page

Abstract

Introduction

Conclusions

References

Tables

Figures



Back

Close

Full Screen / Esc

Printer-friendly Version

Interactive Discussion

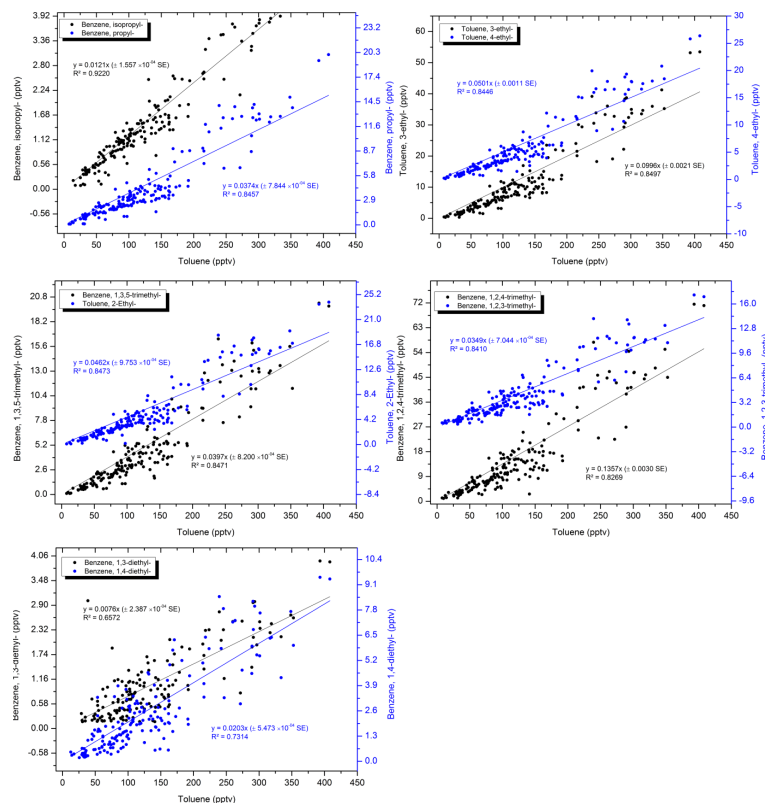


Fig. 5. Plots of monoaromatic mixing ratios from each WAS canister against the simultaneous toluene mixing ratio observed. The coefficient of determination and equations of the linear regressions are also given and are also summarised in Table 3.

An investigation of OH reactivity with monaromatics using GC × GC-TOFMS

R. T. Lidster et al.

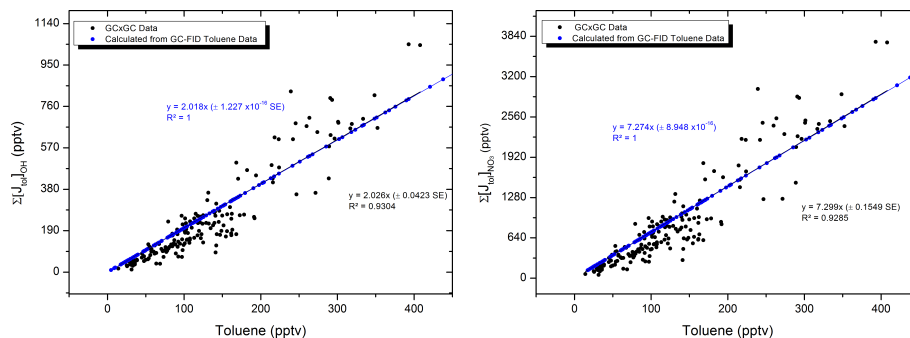


Fig. 6. Measured (black) and predicted (blue) contribution to $[J_{\text{Tol}}]$ for aromatic species measured during RONOCO. Left: Reactivity with respect to OH ($[J_{\text{Tol}}]_{\text{OH}}$). Right: Reactivity with NO_3 ($[J_{\text{Tol}}]_{\text{NO}_3}$). The Blue trace corresponds to a predicted $\Sigma[J_{\text{Tol}}]$ value resulting from a measured toluene mixing ratio from the GC-FID system.

Title Page

Abstract

Introduction

Conclusions

References

Tables

Figures

◀

▶

◀

▶

Back

Close

Full Screen / Esc

Printer-friendly Version

Interactive Discussion

An investigation of OH reactivity with monaromatics using GC × GC-TOFMS

R. T. Lidster et al.

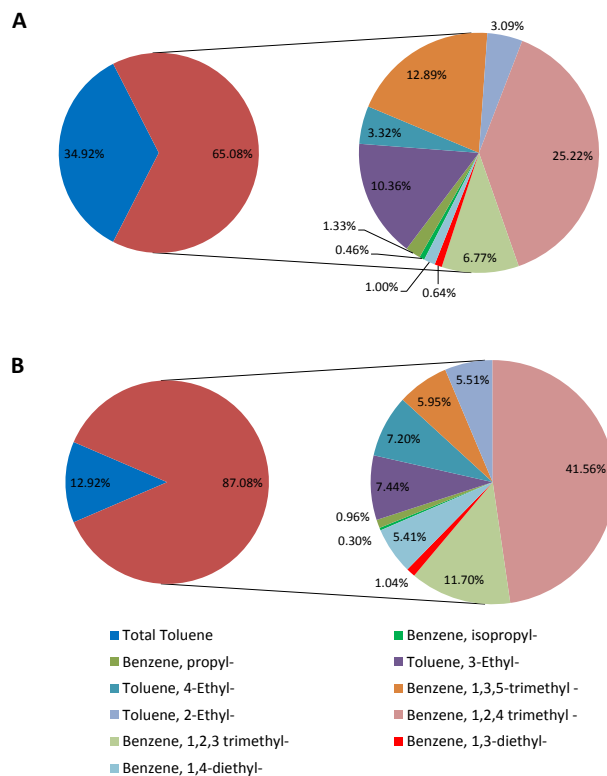


Fig. 7. Monocyclic aromatic species contribution to its corresponding $[J_{\text{Tol}}]$. Red = average $\Sigma[J_{\text{Tol}}]$. Blue = Average toluene mixing ratio. **(A)** = Contribution for reaction with OH ($[J_{\text{Tol}}]_{\text{OH}}$). **(B)** = Contribution for reaction with NO_3 ($[J_{\text{Tol}}]_{\text{NO}_3}$).

[Title Page](#)
[Abstract](#)
[Introduction](#)
[Conclusions](#)
[References](#)
[Tables](#)
[Figures](#)
[Back](#)
[Close](#)
[Full Screen / Esc](#)
[Printer-friendly Version](#)
[Interactive Discussion](#)

An investigation of OH reactivity with monaromatics using GC × GC-TOFMS

R. T. Lidster et al.

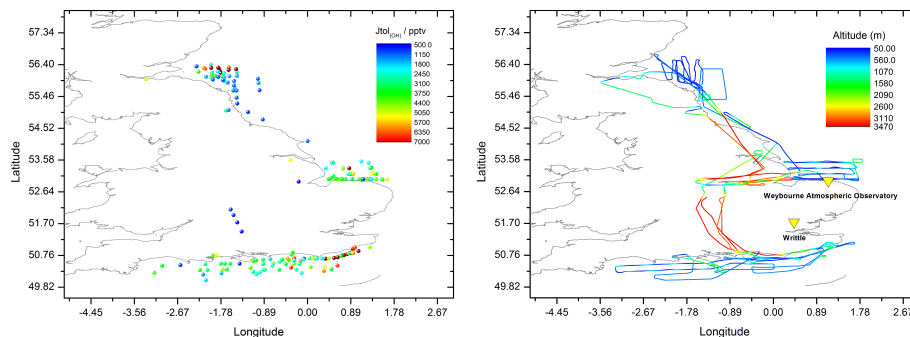


Fig. 8. WAS locations analysed using GC × GC-TOF-MS during the RONOCO campaign. Left: Spatial distribution of WAS bottles, coloured by their respective total $[J_{Tot}]_{OH}$ value. Right: Flight Tracks for the 5 RONOCO flights in which GC × GC-TOFMS analysis was performed, coloured by altitude.

[Title Page](#)[Abstract](#)[Introduction](#)[Conclusions](#)[References](#)[Tables](#)[Figures](#)[◀](#)[▶](#)[◀](#)[▶](#)[Back](#)[Close](#)[Full Screen / Esc](#)[Printer-friendly Version](#)[Interactive Discussion](#)

An investigation of
OH reactivity with
monaromatics using
GC × GC-TOFMS

R. T. Lidster et al.

Title Page

Abstract

Introduction

Conclusions

References

Tables

Figures

◀

▶

◀

▶

Back

Close

Full Screen / Esc

Printer-friendly Version

Interactive Discussion

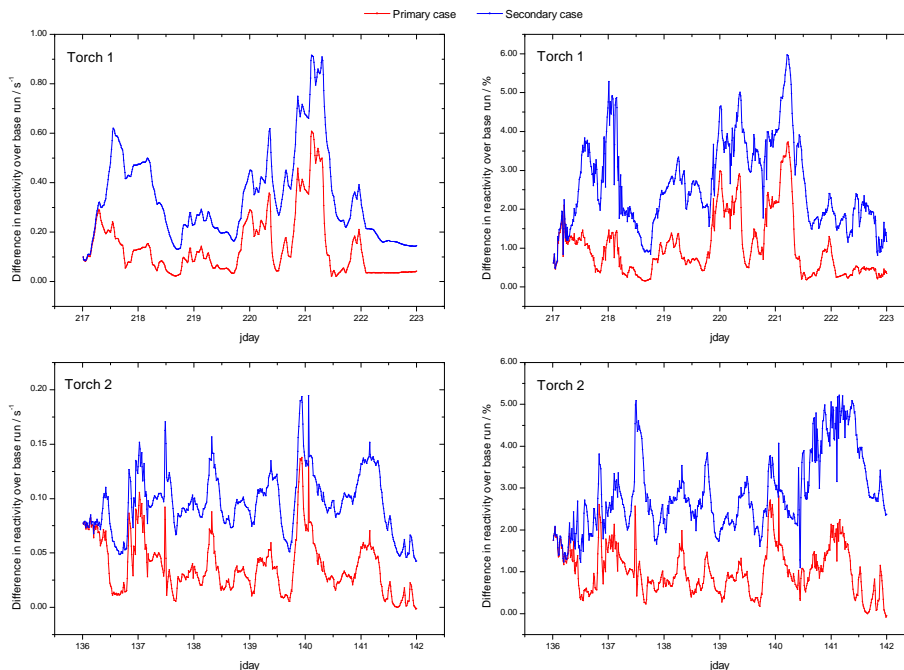


Fig. 9. Modified model data for the TORCH 1 and 2 campaigns. Plots show a difference in reactivity over the original model base case whereby VOC aromatic reactivity has been supplemented using the proportionality factor determined in Fig. 6. The red trace shows the difference between the base case and the primary case which has the additional aromatic content represented by an additional species with the same reactivity as toluene however after initial reaction does not yield further oxidation products. The blue trace shows the difference between the base case and the secondary case where the toluene mixing ratio has been increased to account for the additional aromatic reactivity and secondary reactions are included. Jday = Julian day.

An investigation of OH reactivity with monaromatics using GC × GC-TOFMS

R. T. Lidster et al.

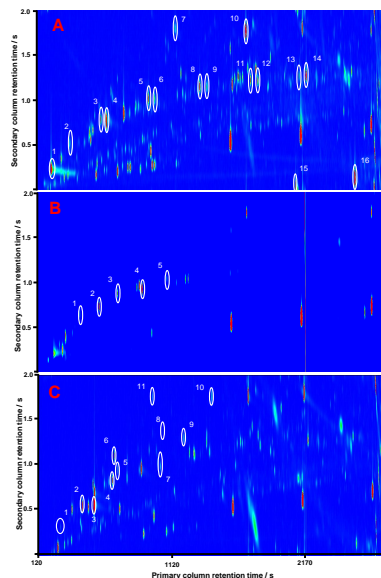


Fig. 10. Typical chromatogram from a sample taken during RONOCO (flight B570 canister 34). **(A)** EIC of m/z 58 + 95 + 112 + 120 + 128, highlighting the presence of oxygenated species. Labelled peaks are identified as follows: (1) acetone; (2) 2-butanone; (3) 2-pentanone; (4) pentanal; (5) 2-hexanone; (6) hexanal; (7) furfural; (8) 2-heptanone; (9) heptanal; (10) phenol; (11) 2-octanone; (12) octanal; (13) 2-nonanone; (14) nonanal; (15) acetophenone and (16) naphthalene. **(B)** EIC m/z 46, highlighting the presence of alkyl nitrate species. Labelled peaks are identified as follows: (1) ethyl nitrate; (2) isopropyl nitrate; (3) propyl nitrate; (4) sec-butyl nitrate and (5) butyl nitrate. **(C)** EIC m/z 63 + 83 + 86 + 93 + 112 + 117 + 166 + 170 + 172 + 174, highlighting the presence of halocarbon species. Labelled peaks are identified as follows: (1) dichloromethane; (2) chloroform; (3) carbon tetrachloride; (4) 1,2-dichloropropane; (5) bromodichloromethane; (6) dibromomethane; (7) tetrachloroethylene; (8) dibromochloromethane; (9) chlorobenzene; (10) tribromomethane and (11) 2-iodopropane.

Title Page

Abstract

Introduction

Conclusions

References

Tables

Figures

◀

▶

◀

▶

Back

Close

Full Screen / Esc

Printer-friendly Version

Interactive Discussion